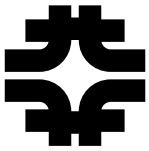

Fermi National Accelerator Laboratory

FERMILAB-Conf-96/043-E
D0

The Top Quark and More: Some Highlights of Physics from the D0 Experiment

Hugh E. Montgomery
Representing the D0 Collaboration

Fermi National Accelerator Laboratory
P.O. Box 500, Batavia, Illinois 60510

February 1996

Presented at the *XVI Encontro Nacional de Fisica de Particles e Campos,*
Caxambu, MG, Brazil, October 24-28, 1995

Disclaimer

The Top Quark and More: Some Highlights of Physics from the DØ Experiment

Hugh E. Montgomery
Fermi National Accelerator Laboratory
P.O. Box 500
Batavia, Il 60510
U.S.A

Representing the DØ Collaboration

Abstract

In this paper we describe some highlights of recent physics results from the DØ experiment at the Tevatron $\overline{p}p$ collider. One aspect of recent QCD experimentation has been the emphasis on studies of events with rapidity gaps; the characteristics of such events in the DØ data are described. The non-abelian nature of the electroweak interaction is a well defined property of the standard model. The very high energies available at the Tevatron have opened a new window which permits the testing of this aspect of the standard model. *THE* highlight among recent results was the observation of the top quark and this result is discussed. At the highest energy available, DØ is conducting numerous searches for phenomena which might indicate the structure of the world beyond the electroweak scale. We discuss searches for the sparticles of supersymmetry. The luminosity of the collider will increase dramatically over the next five years. This will open new fields of investigation for an upgraded DØ detector.

Presented at the XVI Encontro Nacional de Fisica de Particulas e Campos, Caxambu, MG, Brazil, Outubro 24-28, 1995.

1 Introduction

This paper is a description, necessarily brief, of a very few selected topics pertaining to the physics results and the future program of the DØ experiment. It is neither intended to review those results exhaustively[1] nor to make any comparison with results from the other Tevatron Collider experiment, CDF[2]. No attempt is made to update the content for information which has become public since the conference. Nevertheless, I hope that I convey some measure of the excitement of an experiment on the discovery frontier.

DØ is a large international collaboration of more than 400 physicists from 44 institutions worldwide including two Brazilian institutions and three other South American institutions. The DØ detector[3] is shown in Fig. 1. A compact central tracking system is surrounded by a highly segmented liquid Argon and depleted Uranium calorimeter. The calorimeter is in turn surrounded by a muon detection system of solid iron toroids and chambers which together provide identification of muons and a measure of their momenta. Electrons are distinguished from hadrons primarily by the shape of the energy deposition, both in depth and breadth, in the calorimeter and from photons by the presence of an associated track. The acceptance in pseudorapidity extends beyond $\eta = \pm 3$ for the leptons and hadrons. This makes the determination of the missing transverse energy, through the energy imbalance, rather good. It is from this measurement that the transverse energy of a neutrino may be inferred. The detector is thus capable of detecting and measuring the relevant parameters of all the objects resulting from high energy interactions.

In this paper we will first very briefly summarise measurements of the b quark production cross-section. This subject is covered in an extensive parallel session paper at this conference. As an example of an advanced QCD analysis we describe a measurement of even events with substantial regions of rapidity in which there are no particles. Such events have generated interest in the last couple of years both in hadron-hadron collisions and in lepton-hadron collisions. We then discuss diboson production which permits the investigation of the couplings of gauge bosons and in which we have demonstrated the non-abelian nature of the electroweak interaction. In 1995 it would be a sin to omit a description of the observation of the sixth and possibly last quark. The standard model is not thought to be the ultimate description of nature. At DØ we have a program of searches for indications of physics beyond such confines and we will describe a small selection. Finally we will briefly indicate the directions and sensitivities that can be expected from an upgraded detector running with the Tevatron at much higher luminosity in the Main Injector era.

2 Strong Interactions and b Quark Production

The strong interaction is probed in $\overline{p}p$ colliders using many different experimental techniques involving the detection of the different species of quarks and of gluons or generic jets with different multiplicities, or of gauge bosons such as photon or W and Z boson. We confine ourselves to two aspects here.

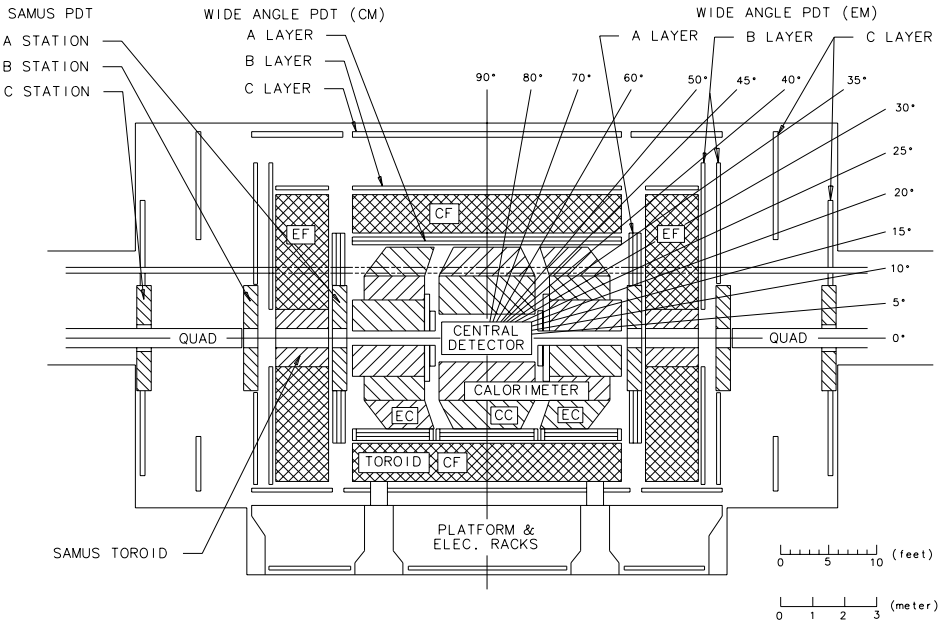

Figure 1: The DØ Detector in a side view showing the location of the component systems.

2.1 b Quark Production

DØ has measured the b quark production cross-section using a number of methods[1, 4, 5]. In general we have used final state muons, in or near jets to indicate the presence of b jets. Backgrounds from π and K decay, and from charm quarks are controlled by the intrinsic properties of the detector and by cuts on the relative kinematics of the detected muons and jets. The subject was covered in considerable detail by Gilvan Alves[5] in a major parallel session presentation at this conference. A comparison of different measurements with the theoretical expectations is given in Figure 2. The data lie somewhat above the central expectations of the theory, but not incompatibly so. The uncertainties on the latter are indicated by the dashed lines.

2.2 Color Singlet Exchange

In this analysis[6, 7] we measure strongly interacting color singlet exchange by tagging events with a low multiplicity of particles between jets. Few particles are expected in the space between the leading jets in color singlet events. In contrast the presence of a color string connecting the scattered partons in color octet events (gluon exchange) gives rise to a smooth distribution of particles between the leading jets. In QCD the absence of particles as a result of strong color singlet exchange is a manifestation of the destructive interference between the emissions of gluons from two colored objects, the gluon components of the pomeron.

Two different data sets were used to study this effect: one selected events with the two jets on opposite sides, in η, of the calorimeter ($\eta_1 \cdot \eta_2 < 0$) while the other selected events with jets on the same side ($\eta_1 \cdot \eta_2 > 0$). The same side sample is expected to be dominated by color octet exchange and is used as a control. Figure 3 shows the number of electromagnetic

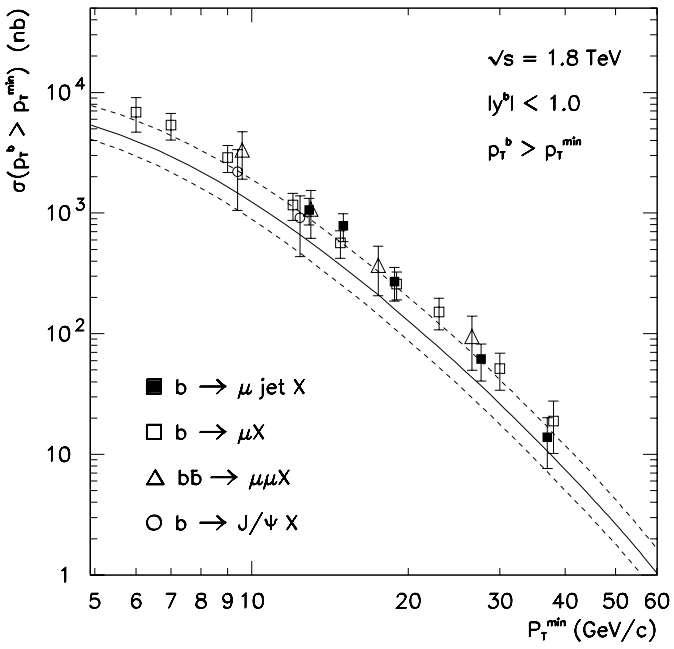

Figure 2: b-quark production cross sections for $\mid y^b \mid < 1$ from the inclusive muon, muon plus jet, dimuon and J/ψ data samples.

calorimeter towers above threshold (n_{cal}) versus the number of central drift chamber tracks (n_{trk}) for the (a) opposite side and (b) same side samples. Each of these measures is sensitive to a different fraction of the total particles produced. The two distributions are similar in shape except at very low multiplicities, where the opposite side sample has a striking excess of events in the region where the multiplicity of both electromagnetic calorimeter cells, and tracks is close to zero. One can perform fits in one or other of these variables. Except for the lowest bins, the multiplicities are well described by negative binomial distributions, or modified negative binomial distributions. In the opposite side sample there is an excess in the low multiplicities consistent with the existence of a color singlet exchange process. We measure the fractional excess of color singlet above color octet exchange to be 1.07 ± 0.10 (stat) $^{+0.25}_{-0.13}$ (syst)%. The probability of such an excess has been estimated for both electroweak and strong color singlet (pomeron) exchange. The former is expected to be at a level much below that observed. On the other hand, the estimations for pomeron exchange are at approximately the level observed.

3 Electroweak Interactions: The Boson Couplings

Tests of the electroweak sector of the Standard Model have concentrated on the consistency between, and the radiative corrections to, the basic parameters of the model. One aspect which has received relatively little attention until recently is the examination of the vertex functions, the couplings between the vector bosons themselves. The very fact of their mutual interaction is a feature of the non-abelian nature of the theory which in turn is related to

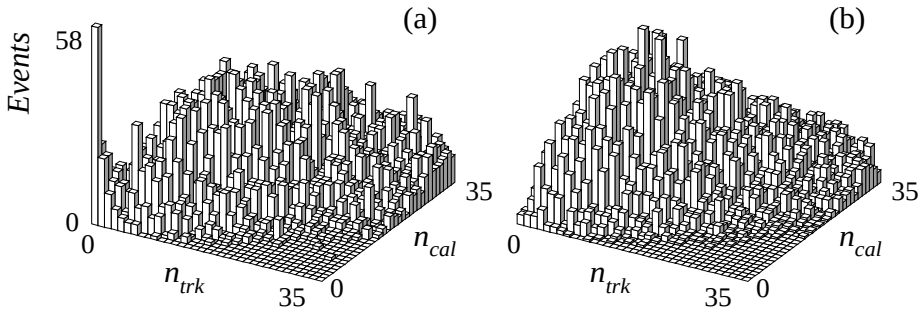

Figure 3: The calorimeter tower multiplicity (n_{cal}) vs. the charged track multiplicity (n_{trk}) in the pseudorapidity region $|\eta| < 1.3$ for the (a) opposite-side and (b) same-side samples described in the text.

its local gauge invariance. A straightforward way to examine such interactions is through the production of pairs of gauge bosons. Given the high masses of the W and Z, there is a premium on high energy. Consequently the advances from the Tevatron data have been remarkable.

3.1 Diboson production

In the standard electroweak model, the self-couplings of the W, Z, and γ bosons are completely specified and so consequently, are the gauge boson pair production cross sections. $W\gamma$[8], $Z\gamma$[9], WW[10] and WZ[11] production have all been studied by DØ . The ZZ production cross section is extremely small.

The production mechanisms include both t-channel quark exchange diagrams and the direct s-channel diagram with a third virtual vector boson in that channel. The latter diagram involves the trilinear vector boson couplings. Deviation from the standard model predictions could imply new physics entering through loop corrections to this vertex. Any non-Standard Model contributions to the $WW\gamma$ vertex, can be interpreted as an anomalous contribution to the electromagnetic dipole and quadrupole moments of the W. This is analogous to the contributions to $g-2$ of the muon from the "new physics" in the weak and hadronic loop diagrams.

A useful feature from the experimental point of view is that any anomalous couplings enter quadratically in the expression for the cross section and hence would lead to an increase in the cross section. A limit measurement therefore necessarily constrains the anomalous components. In addition the enhancement occurs with a weaker dependence on p_T than the standard form so that examination of the p_T dependence of any observed signal provides further discrimination.

Generally, each trilinear vertex can be described by a set of four coupling constants. The $WW\gamma$ (WWZ) couplings are usually referred to as $\kappa_{\gamma(Z)}$, $\lambda_{\gamma(Z)}$, $\tilde{\kappa}_{\gamma(Z)}$, $\tilde{\lambda}_{\gamma(Z)}$, with the first two couplings being CP-conserving and the other two being CP-violating. For $ZZ\gamma$ ($Z\gamma\gamma$) vertices the corresponding couplings are denoted $h_i^{Z(\gamma)}$, $i = 1...4$, with $h_{1,2}$ being CP-violating and $h_{3,4}$ CP-conserving. In the Standard Model $\kappa_{\gamma,Z} = 1$; all others are zero. The

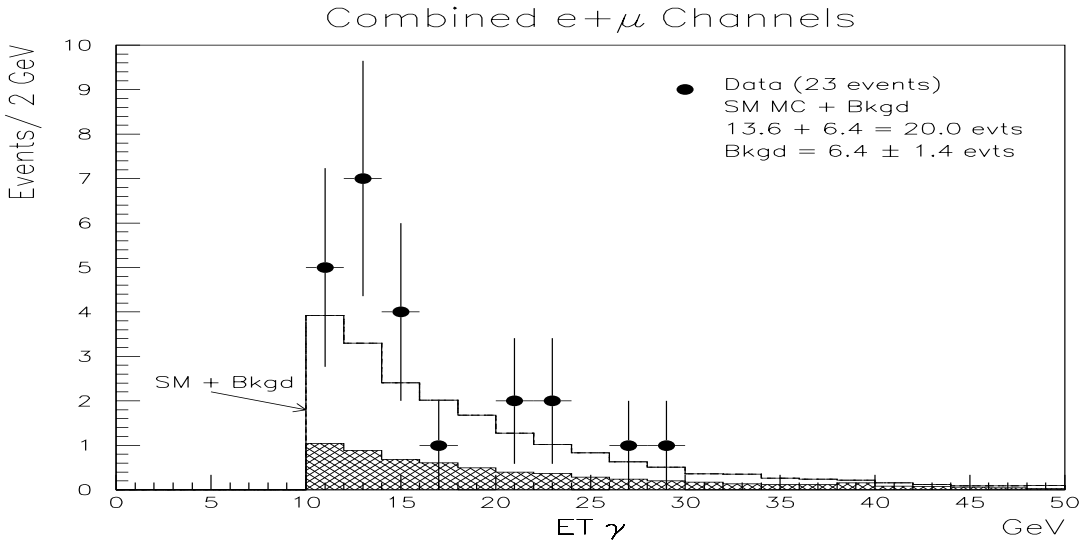

Figure 4: Transverse energy spectrum of the photon produced in $p\bar{p} \to W\gamma + X \to \ell\nu\gamma + X$, $\ell = e, \mu$. The points are data, the shaded area represents the estimated background, and the solid histogram is the sum of the SM prediction and estimated background.

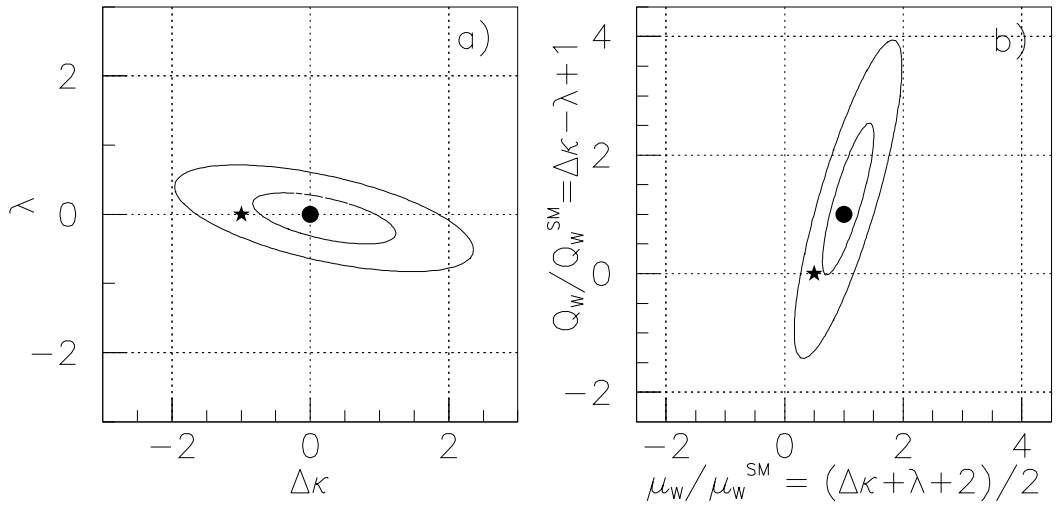

Figure 5: Limits on (a) *CP*-conserving anomalous coupling parameters $\Delta\kappa$ and λ, and on (b) the magnetic dipole μ_W and electric quadrupole Q_W^e moments of the W boson. The ellipses represent the 68% and 95% CL exclusion contours. The dot represents the SM values, while the star indicates the $U(1)_{\mathrm{EM-only}}$ coupling of the W boson to a photon. Form-factor scale $\Lambda = 1.5$ TeV.

convention $\Delta\kappa = \kappa - 1$ will be used below.

The admission of non-standard values for the couplings is an ad hoc procedure and does not necessarily lead to a consistent theory. In particular, unless modifications through form factors with scale Λ are introduced, S-matrix unitarity is violated at high sub-process energies. A simplified way to look at the plotted unitarity bounds, Fig. 6, is to consider that if the measured limits fit within the bound for a higher Λ, they are more stringent than if they fit only within the bound for a smaller Λ. As the limits approach more closely the

standard model values, the Λ scale, which can be accommodated, approaches infinity.

Using $W\gamma$ production data with both electron and muon decays of the W, the γ transverse energy distribution is shown in Fig. 4, there are 23 candidates and a background of 6.4 ± 1.4 events. The corresponding limits are shown in Fig. 5 for both 68% and 95% confidence level. The star indicates the expectation for purely electromagnetic coupling of the W and photon, and a gyromagnetic ratio of unity for the W boson. Thus, at 80% confidence level, the weak-electromagnetic unification of the couplings is required.

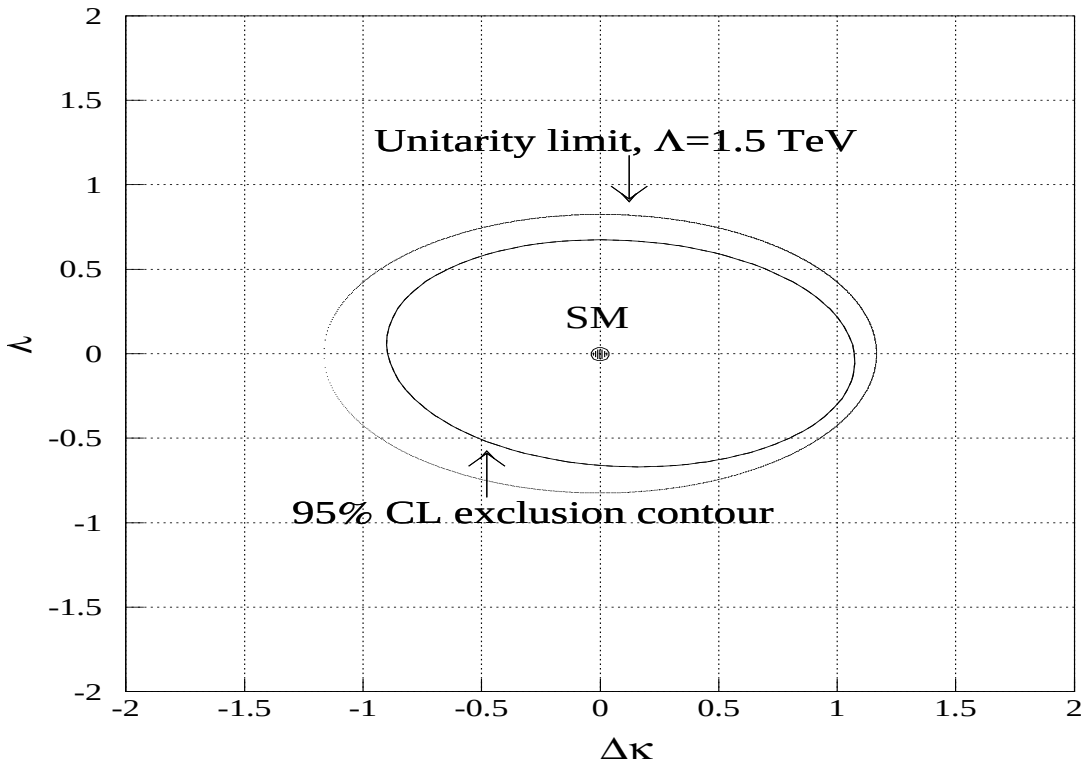

Figure 6: 95% CL limits on the *CP*-conserving anomalous couplings $\Delta\kappa$, λ assuming $\Delta\kappa_\gamma = \Delta\kappa_Z; \lambda_\gamma = \lambda_Z$ derived from $WW/WZ \to e\nu jj$. The dashed line shows the S-matrix unitarity limits. Form-factor scale $\Lambda = 1500$ GeV.

In the $Z-\gamma$ final state six events are observed with an expected background of 0.48 ± 0.06 events and a fit to the transverse momentum spectrum of the γ is used to obtain limits. For WW production only one candidate is observed with an expected background of 0.56 ± 0.13 events. Besides the lepton-only channels, one can look for the case where one of the bosons decays into a pair of hadronic jets. Again the transverse momentum of the objects is a key discriminator. The limits obtained are shown in Fig. 6. In this case a unitarity bound of 1.5 TeV can be accommodated by any values of the coupling constants in the allowed region.

The limits resulting from these analyses are collected in Table 1. The corresponding CP-violating limits in all the above analyses the limits are numerically the same. With this rather large number of independent measurements available, and with comparable sensitivity, the next step will be to combine the limits and obtain an overall constraint on the deviations of the couplings from the standard model expectations.

CP-conserving coupling limits		Channel
$-1.6 < \Delta\kappa_\gamma < 1.8$,	$-0.6 < \lambda_\gamma < 0.6$	($W\gamma$, $\Lambda = 1500$ GeV)
$-1.8 < h_{30}^Z < 1.8$,	$-0.5 < h_{40}^Z < 0.5$	($Z\gamma$, $\Lambda = 500$ GeV)
$-1.9 < h_{30}^\gamma < 1.9$,	$-0.5 < h_{40}^\gamma < 0.5$	($Z\gamma$, $\Lambda = 500$ GeV)
$-2.6 < \Delta\kappa_\gamma = \Delta\kappa_Z < 2.8$,	$-2.1 < \lambda_\gamma = \lambda_Z < 2.1$	($WW \to \ell^+\ell^-\nu\nu$, $\Lambda = 900$ GeV)
$-0.9 < \Delta\kappa_\gamma = \Delta\kappa_Z < 1.1$,	$-0.7 < \lambda_\gamma = \lambda_Z < 0.7$	($WW/WZ \to e\nu jj$, $\Lambda = 1500$ GeV)

Table 1: Limits on the CP-conserving couplings. Limits for the CP-violating couplings are the same within 5%.

4 The Top Quark

4.1 Observation of the Top Quark

In the spring of 1995, CDF[12] and DØ[13] published papers describing the observation of the top quark. The high top mass had retarded progress[14] but led to a clear experimental signature. Two large mass objects decay each into a W boson and a b quark. In turn, the former can decay either leptonically or hadronically, the latter results in a jet in which there may be an embedded muon as a result of the semi-leptonic decay of the b or its daughter c quark. If both W bosons decay leptonically a final state with two high p_T, isolated charged leptons and two jets results. If one of the W bosons decays hadronically there are 4 jets in the final state. The former case is generically labelled "dilepton", the latter "lepton plus jets". In both cases there is substantial missing transverse energy as a result of the presence of one or more neutrinos.

In the dilepton case the backgrounds are dominantly physics processes which can lead to the same final states. For example Z production leads to $\mu\mu$ and ee final states.

In the case of the lepton plus jets channels the dominant backgrounds are those with a real or false W boson and multiple jets. The false W boson is generated by mis-identification of one of the jets in a multi-jet event in conjunction with a mismeasurement of the missing transverse energy. To reduce the background two approaches are used.

One approach applies kinematic cuts to the observed events such as to reduce the W-plus-jets background while maintaining acceptance for top production. The event shape for top is typically spherical with all objects having large transverse momenta. The W-plus-jets background tends to derive several of its jets due to gluon radiation from a primary two parton final state configuration. The planar characteristics of that two-body state often survive, even after gluon radiation, since the radiated jets tend to be at low relative transverse momenta.

The second approach relies on the presence of two b jets in top events. The probability that a muon from either direct or cascade decays of one or other of these b jets exists is about 45% . The probability that the μ is detected in DØ is about 50% , so about 22% of top events should have an observed soft muon. In contrast, the probability that a generic mixture of jets will lead to the same is approximately 0.5% per jet (dependent on jet p_T). The jet μ tag rate has been measured using various samples of data and, at the level of

Decay Mode	Number of Events	Background	Significance
Dilepton	3	0.65 ± 0.15	0.03 (1.9σ)
Lepton plus jets (topological)	8	1.9 ± 0.5	0.002 (2.9σ)
Lepton plus jets (b–tag)	6	1.2 ± 0.2	0.002 (2.9σ)
All	17	3.8 ± 0.6	2.0×10^{-6} (4.6σ)

Table 2: The number of events observed, background predicted, and the probability that the background fluctuated up to the observed data for each channel.

precision needed, is independent of the data sample. It is therefore taken to be true for both the principal backgrounds, true and false W bosons with multiple jets.

The observed numbers of events are summarized in Table 2. Also shown is the predicted background for each $t\bar{t}$ decay channel along with the probabilities for the predicted background to fluctuate up to account for the observed data. The combined probability that the observed events be a background fluctuation is

$$\mathcal{P} = 2.0 \times 10^{-6}.$$

The corresponding cross-section, for a top quark of mass m_t= 200 GeV/c^2, is $\sigma_{t\bar{t}} = 6.3 \pm 2.2$ pb. These results were based on an integrated luminosity of about 50 pb^{-1}.

4.2 Top Quark Mass

In the simplest situation the final state with $t\bar{t}$ consists of six final state fermions. There are therefore 18 momentum components to be determined. Under the $t\bar{t}$ production hypothesis there are two constraints from the known W masses and a further constraint from the equality of the masses of the t and $\bar{t}$. Provided that the different decay components are unambiguously identified, fifteen of the momentum components must be measured to completely describe the event. With more, a constrained fit for the mass of the top can be attempted.

4.2.1 The Lepton plus Jets Channel

In the lepton plus jets channel, an attempt is made to identify the the decay $t\bar{t} \rightarrow \ell\nu b\ q\bar{q}\bar{b}$. This demands at least four quark jets in the event. Complications can arise since primary quark jets may escape detection, be merged with other jets, or jets arising from gluon radiation may increase the jet multiplicity. The momenta of the four most energetic jets, the lepton, and the missing energy, for which we measure only the two transverse components, give a total of 17 measurements. If the b jets are not identified the number of possible permutations of assignments is twelve. Taking into account the ambiguity for the longitudinal momentum of the neutrino gives a total of 24 possible combinations for each event.

With the mass constraints, a fit to the $t\bar{t}$ system is performed. We apply a cutoff in the fit quality (χ^2); events which do not have a jet assignment combination with a χ^2 below the cutoff are dropped from the m_t results. Finally, the central mass is obtained from the

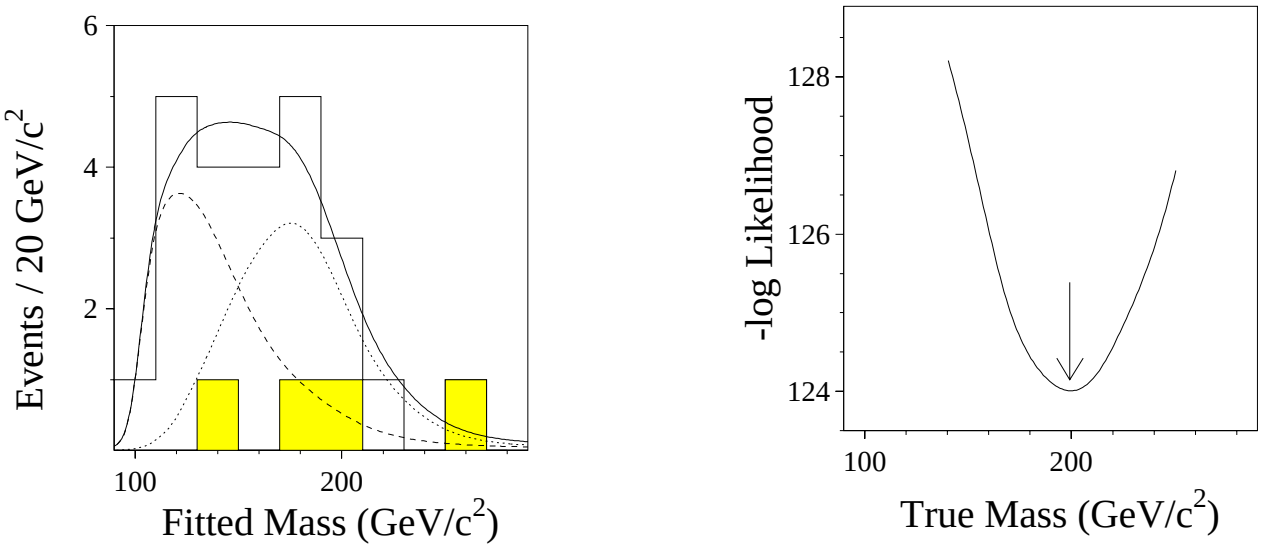

Figure 7: The fitted mass distribution (a) for events is shown as the line histogram, the dashed line is the background distribution and the dotted line is the best fit Monte Carlo fitted mass distribution. The solid line is the combination of the best fit Monte Carlo plus background. The shaded histogram represent events that were bottom quark tagged. The top mass is extracted from the fitted mass distribution using a likelihood method (b).

weighted average of the best three χ^2 fits for each event. The result is termed the 'fitted mass'.

A number of template distributions from a $t\bar{t}$ Monte Carlo are generated for a range of top masses and for each distinct decay channel. A similar template is prepared for the background processes. All detector effects and biases from the fitting procedures are accounted for by the simulation. The top mass is then obtained using a likelihood fit of the signal and background templates to the observed distribution of fitted masses.

The result is:

$$m_t = 199^{+19}_{-21}(\text{stat})^{+14}_{-21}(\text{syst})\ \text{GeV/c}^2$$

Jet combinatorics contribute strongly to the bias in mapping between observed and true masses and also to the width of that distribution. This and other effects were extensively examined using Monte Carlo studies and are included in the systematic error assignment.

Figure 7(a) shows the fitted mass distribution for the DØ lepton plus jets events, taken with loose selection criteria. The histogram represents the fitted masses of the observed events, and the solid curve represents the background and the top Monte Carlo combined. Figure 7(a) is the distribution of central mass values, Fig. 7(b) shows the resulting likelihood fit, with an arrow indicating the best fit value. Note that the clear separation of background and signal events, permits a good top mass determination.

4.2.2 The Dilepton Channel

The dilepton channel is more difficult as we have less information, an extra neutrino in the final state reduces the constraints by three. In order to provide additional information, a

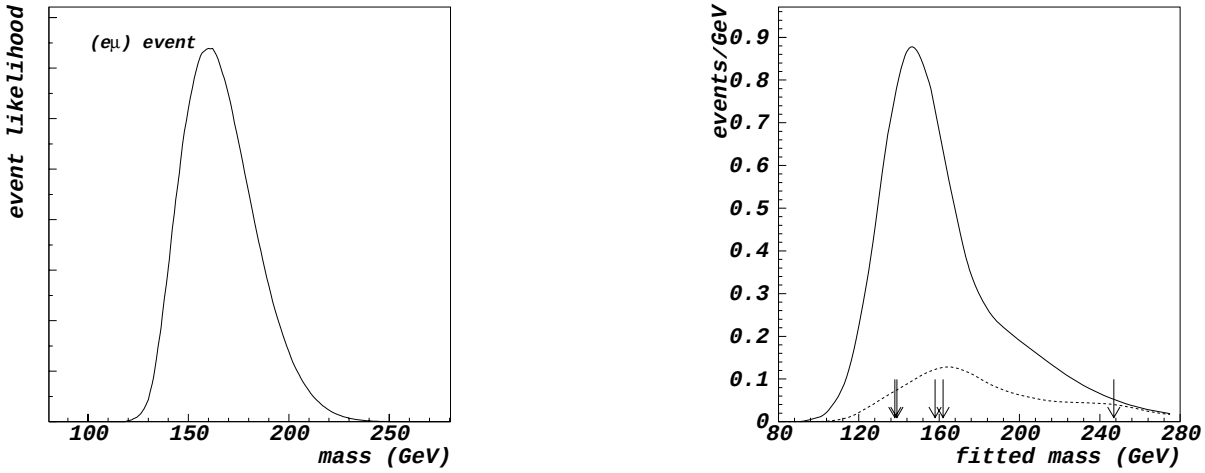

Figure 8: The dilepton mass fit method. The likelihood as a function of top mass for a particular event is shown in (a). The peak represents one of the arrows in (b), which is the fitted mass for all the dilepton events (arrows). The background fitted mass distribution is shown as the dashed line, and the best fit for background and Monte Carlo is shown as the solid line. The likelihood curve for the best mass has a broad minimum (not shown), leading to large errors on the mass.

model of the initial state parton momentum distributions and the expected decay characteristics of the standard model top quark are used.

We use a method[15] inspired by Dalitz, Goldstein and Kondo[16], but which takes into account all the measured information and reduces the theoretical assumptions. For a given event a top quark mass is chosen and a weight is assigned and based on known distributions of the transverse momentum of the lepton and the distribution functions for the valence quarks. The result is a likelihood curve for each event as a function of m_t, as shown in Figure 8(a). Analogously to the lepton plus jets analysis, the most likely value of mass is retained as a characteristic parameter for each event.

Templates for the distributions of most likely masses are prepared from $t\bar{t}$ Monte Carlo and background samples. The best true mass is extracted using a likelihood method analogous to that used in the lepton plus jets analysis. Figure 8(b) shows the resulting best fit, where the arrows denote the peak of each individual event's likelihood curve, the dashed histogram is the background Monte Carlo distribution, and the solid is the fit for the best value of the true mass. The likelihood is broad, and gives the result:

$$m_t \approx 145 \text{ GeV/c}^2 \text{ (preliminary)}$$

The statistical error deduced by examining the behavior of Monte Carlo samples of the same size is 25 GeV/c^2 , the systematic error is approximately 20 GeV/c^2, dominated by jet energy resolutions.

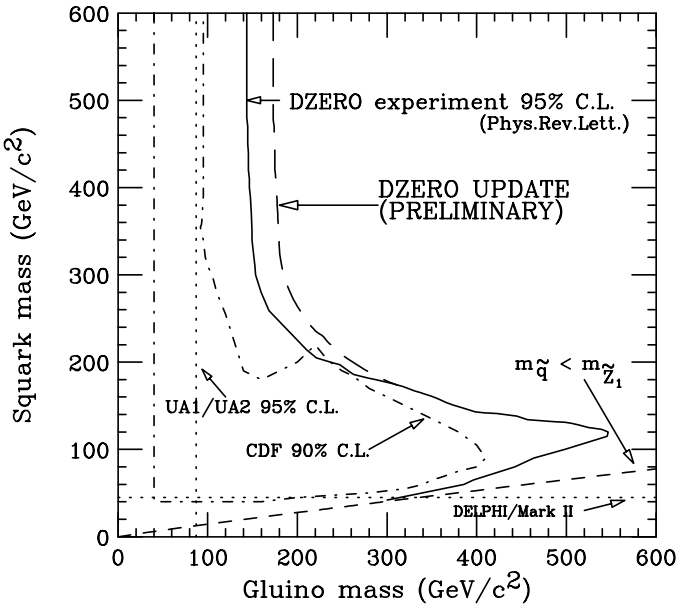

Figure 9: The squark and gluino mass limits. The long dashed line marks the *preliminary* DØ 95% confidence level excluded region from the combination of the three jet and four jet analyses. The solid line indicates the DØ three jet search result. The region below the dashed line labeled $m_{\tilde{q}} < m_{\tilde{Z}_1}$ is excluded since there the squark becomes lighter than the LSP. Other published limits from CDF, UA1, UA2, and DELPHI are displayed as well.

5 Beyond the Standard Model: SUSY Searches

Although the standard model is a useful framework, the search for physics beyond the standard model is a necessity for the highest energy experiments.

Supersymmetric extensions of the standard model, which relate bosons and fermions, are theoretically attractive. However they lead to a second array of fundamental particles dubbed "sparticles" . In the *Minimal Supersymmetric Standard Model* , unstable sparticles must decay into a lighter sparticle (plus other ordinary particles); there must then be one sparticle which does not decay. This is referred to as the LSP. Most models have the $\tilde{Z}_1$ as the LSP.

5.1 Squarks and Gluinos

The most copiously produced SUSY particles should be squarks ($\tilde{q}$) and gluinos ($\tilde{g}$). In previous searches, the $\tilde{q}$ and $\tilde{g}$ were assumed to decay directly into quarks and the lightest supersymmetric particle. The event signature for which we have searched[17] is three or more jets and missing transverse energy ($\not\!\!E_T$). One measurement searched for events with three or more high E_T jets and very large $\not\!\!E_T$, and another for events with at least four jets but slightly less $\not\!\!E_T$.

The major backgrounds to these searches are vector boson production with associated jets and QCD events with mismeasured jet energies. After analysis cuts, 14 events survived in the three jet analysis and 5 events in the four jet sample.

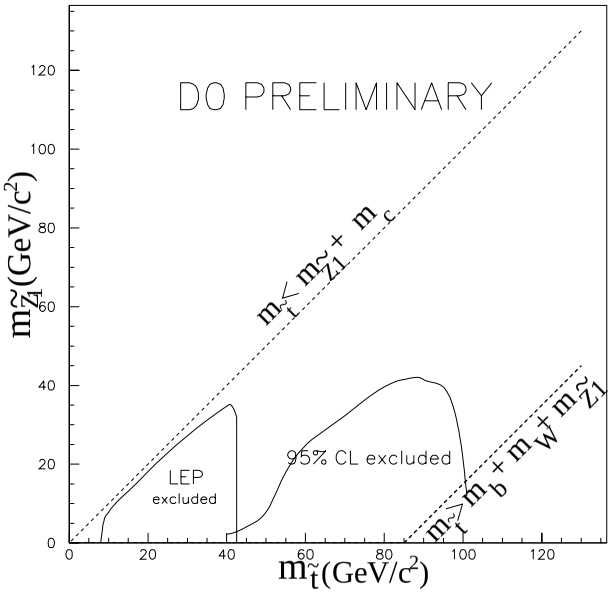

Figure 10: The DØ 95% Confidence Level top squark exclusion contour. Also shown is the result from LEP (OPAL experiment).

Backgrounds from vector bosons plus jets backgrounds were estimated. The detector response was simulated using the DØ detector simulation program. A total of 14.2 $\pm$ 4.4 W/Z events are expected to pass the three jet analysis cuts. For the four jet search, 5.5 $\pm$ 2.2 events are predicted. The contribution from multijet production was estimated using data from jet triggers. We predict 0.42 $\pm$ 0.37 events for the three jet analysis and 1.6 $\pm$ 0.9 events for the four jet search.

Since the number of events seen in the squark/gluino data sample is consistent with these standard model backgrounds no signal is observed. 95% CL lower mass limits of $m_{\tilde{g}} > 173$ GeV/c^2 for large squark mass, $m > 229$ GeV/c^2 for the case of equal mass squarks and gluinos, are obtained. The limits are shown in Fig. 9

5.2 The Top Squark

The squark/gluino search assumed that the squarks are mass degenerate. The large top mass can drive the mass of its SUSY partner, the top squark or stop ($\tilde{t}$) to lower masses than the other squarks. Mixing between the left- and right-handed top squarks can also leave one of the two $\tilde{t}$ lighter than the top quark itself. A light top squark mass is popular in view of recent measurements of the $Z \to b\bar{b}$ branching fraction at LEP[18].

The top squark[19] is expected to decay via $\tilde{t}_1 \to b\tilde{W}_1$. If $m_{\tilde{W}_1} > m_{\tilde{t}_1} + m_b$ the three-body decays $\tilde{t}_1 \to bl\tilde{\nu}$ and $\tilde{t}_1 \to b\nu\tilde{l}$ will predominate *unless* sleptons and sneutrinos are also much heavier than the $\tilde{t}_1$. In this second case the top squark will decay via $\tilde{t}_1 \to c\tilde{Z}_1$ producing final states with two acollinear jets and $\not\!\!E_T$. In either case, the expected signature of the top squark events is two energetic jets and large $\not\!\!E_T$ from the two LSP's.

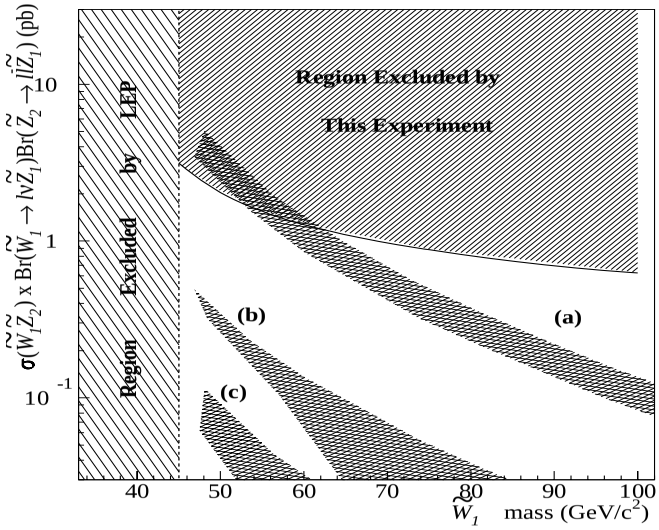

Figure 11: The 95% CL limit on cross section times branching ratio into any one trilepton final state, as a function of $m_{\widetilde{W}_1}$, along with the region of $m_{\widetilde{W}_1}$ excluded by LEP. Also shown are bands of theoretical predictions, as described in the text.

The top squark production occurs via gluon fusion and $q\bar{q}$ annihilation and is thus fixed by QCD in terms of $m_{\tilde{t}_1}$. The decay topology is solely determined by $m_{\tilde{t}_1}$ and $m_{\tilde{Z}_1}$. Our background subtracted 95% CL exclusion limit contour is shown in Fig. 10. This contour intersects the $m_{\tilde{t}_1} = m_{\tilde{\chi}_1^0} + m_b + m_W$ line at $m_{\tilde{Z}_1} = 8$ GeV/c^2 and $m_{\tilde{t}_1} = 93$ GeV/c^2, the highest $m_{\tilde{t}_1}$ value we exclude. The maximum excluded value for $m_{\tilde{Z}_1}$ is 44 GeV/c^2 for $m_{\tilde{t}_1} =$ 85 GeV/c^2.

5.3 Gaugino Searches

The largest gaugino production cross section is for a $\widetilde{W}_1\tilde{Z}_2$ pair. The decays of the $\widetilde{W}_1$ and $\tilde{Z}_2$ can lead to final states similar to those from virtual W and Z bosons plus missing E_T from the LSP's. The possible event signatures are: four jets + $\not\!\!E_T$, lepton + two Jets + $\not\!\!E_T$, two leptons + two jets + $\not\!\!E_T$, and three leptons + $\not\!\!E_T$. The last channel has few standard model backgrounds and is relatively clean in terms of hadronic activity. We see no candidate events[20] consistent with $\widetilde{W}_1\tilde{Z}_2$ pair production and subsequent decay into trilepton final states.

Detection efficiencies were determined using a combination of data and Monte Carlo simulations. The main sources of background are single lepton and dilepton events with one or more misidentified leptons. These were estimated from data and Monte Carlo.

The results from the four channels trilepton channels were combined in the calculation of the limit, with the assumption that $BR(eee) = BR(ee\mu) = BR(e\mu\mu) = BR(\mu\mu\mu)$. In Fig. 11 we show the resulting 95% c.l. limit in the region above the LEP limit. For comparison, we also show three bands of theoretical curves. Band (a) shows the ISAJET production cross section obtained with a wide range of input parameters, multiplied by a branching ratio of $\frac{1}{9}$. The value of $\frac{1}{9}$ for a single trilepton channel is obtained when the $\widetilde{W}_1$ and $\tilde{Z}_2$ decay purely leptonically. Branching ratios of this order are predicted in models with very

light sleptons. Bands (b) and (c) show the $\sigma \cdot BR$ values from ISAJET obtained with the unification scale parameters $m_0 = [200, 900]\mathrm{GeV/c^2}$, $m_{\frac{1}{2}} = [50, 120]\mathrm{GeV/c^2}$, $A_0 = 0$ and the sign of μ negative. Band (b) is for $\tan\beta = 2$ and band (c) for $\tan\beta = 4$.

6 Future Prospects

The approved DØ upgrade retains the strengths of the existing detector, including hermetic coverage in finely segmented liquid argon calorimetry and large acceptance muon detection using magnetized iron toroids, and combines these with a new magnetic central tracking system based upon scintillating fibers and silicon strip technologies in a 2 Tesla solenoidal field.

The Tevatron Collider Luminosity has increased tenfold between 1989 and 1996. The Main Injector is currently under construction and a further factor of ten may be anticipated by the first years of the next decade. Initial running, starting in 1999 with the new machines, is expected to yield an integrated luminosity of $2pb^{-1}$. This would be about a factor twenty more than the current data sample and opens new windows on physics.

6.1 Components of the DØ Upgrade

A key element of the upgraded DØ detector is the introduction of a 2 Tesla solenoidal field to enable improved b quark tagging and to provide added calibration and precision for lepton measurements. The central tracking region is instrumented with several new detector systems. Surrounding the collision region at radii less than 10 cm and covering $|\eta| < 3$ is a silicon vertex tracker.

Surrounding the silicon tracker is a central scintillating fiber tracker which covers the radial interval $20\,\mathrm{cm} < \mathrm{r} < 50\,\mathrm{cm}$, and pseudorapidity interval $|\eta| < 2$. The scintillating fibers are 830 μm in diameter and are read out with light sensing visible light photon counters (VLPC's). This leads to a compact fast tracker with high efficiency, good resolution, and excellent trigger and pattern recognition capabilities.

The present liquid argon calorimetry system is expected to operate very well at the proposed luminosities after upgrade of the readout electronics. The effects of pileup due to the shorter Tevatron bunch crossing times will be offset by new, lower noise, front end electronics and reduced sampling times. The existing intercryostat detector will be reworked to operate in a magnetic field.

The iron toroids and the drift chambers for the central muon system will be retained, but the front-end electronics for the chambers will be modified. For the region $|\eta| < 1$, new scintillation counters will be installed to reduce the muon trigger p_T threshold to about 1.5 GeV/c. For $1 < |\eta| < 2.2$, new scintillator and "pad-pixel" proportional drift tube chambers will be installed.

The multi-level trigger system will be reworked to increase the flexibility and the bandwidth and help reduce the rates as the luminosity increases. Some of this upgrade will involve completely new filtering and data acquisition software. The world of computing has evolved tremendously since the original design of DØ and fitting the old and new analysis code into

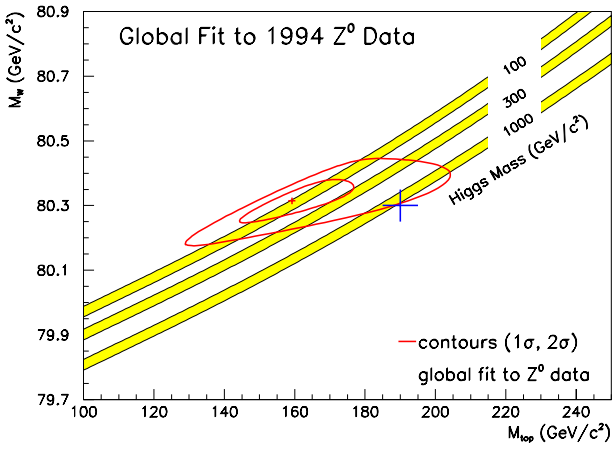

Figure 12: m_t–m_W contours from a global standard model fit to all e^+e^- and νN data, with m_h a free parameter. A hypothetical Run II measurement is shown.

a framework of Object Oriented software is one of several areas where we expect the LAFEX group to play a major role.

6.2 The DØ Upgrade Physics Program

A central goal of the upgraded DØ program is the substantial improvement of our knowledge of the standard model electroweak parameters. Measurement of the top quark and W boson masses to much better precision than available now will be possible and will permit incisive tests of the validity of the model and indirectly constrain the Higgs boson mass. The study of forward-backward asymmetries in Z leptonic decays will also complement the precision information from LEP on heavy quark and leptonic asymmetries and will provide high precision information on $\sin^2\theta_W$ for light quarks. These measurements will allow consistency checks of the standard model within a single experiment, complementary to the direct searches for new phenomena, which will continue to be a major part of the DØ high p_T physics program.

A reconstructed sample of ~ 1000 $t\bar{t}$ candidates is expected with a signal to background ratio of $> 5:1$. With this sample, one can measure m_t to a precision of better than 5 GeV/c^2, corresponding to an uncertainty in the SM Higgs mass of $\delta m_h/m_h \sim 0.8$. Roughly half of the uncertainty in m_t is of statistical origin, and the remainder is due to systematics such as uncertainties in the energy scale and in Monte Carlo simulation of the effects of gluon radiation. The presence of W decays to two jets in the top decays themselves offers a powerful tool for *in situ* calibration of the multijet mass scale.

Improved measurements of the W boson mass m_W (accompanied by a measurement of m_t) provides a constraint on the Higgs mass as shown in Fig. 12. For e and μ channels, a W mass measurement with $\delta m_W = 40\,\mathrm{MeV/c^2}$ is expected.

We will also be able to begin the Higgs search in the WH^0 channel in the mass region near 100 GeV/c^2. Table 3 contains a summary of current and future possible search limits

Possible signals	Production cross sections (over accessible mass range)	Mass limit (model dependent)	Discovery reach $1\ \mathrm{fb}^{-1}$
$t\bar{t}$	6.3 ± 2.2 pb	199 ± 30 GeV (measured)	discovered!
W_R	0.5-1000 pb	720 GeV	
W'	0.5-0.0001 x σ_W	610 GeV	~ 1 TeV
Z'	0.1-0.001 x σ_Z	480 GeV	~ 1 TeV
scalar 1st generation leptoquarks	1.0-100. pb	133 GeV	~ 240 GeV
scalar 2nd generation leptoquarks	1.0-100. pb	119 GeV	~ 240 GeV
$\tilde{q}$ and $\tilde{g}$ pairs	5-1000 pb	170-230 GeV	~ 200-320 GeV
gaugino pairs	0.5-10.0 pb	~ 60 GeV[a]	~ 90 GeV
$\tilde{t}$	0.1-100 pb	~ 90 GeV [b]	
b'	10-1000 pb	not yet reported	
q^*	0.1-100 pb	not yet reported	~ 700 GeV

[a] sleptonic-dominated decays
[b] heavy $\widetilde{W}$, slepton

Table 3: Summary of DØ's current limits and mass reach for the discovery of new particles (10 events required for discovery).

from DØ[1].

The approved upgrade DØ detector provides a versatile experimental platform with significant capabilities for the study of top, electroweak symmetry breaking, QCD, b-physics, and new phenomena. The upgrade maintains the excellent performance characteristics of the present detector and significantly improves the capabilities for b-tagging, and electron, muon and tau identification and measurement. The detector is well matched to the accelerator environment and the physics goals and provides a solid foundation for any additional enhancements needed for operation at higher luminosities.

7 Conclusions

Over the last year or so, DØ has observed the top quark, has numerous interesting results in the basic standard model physics that rules our everyday lives and has shown several unique results of searches for the most likely of possible extensions of the standard model. In particular SUSY scenarios have received some concerted attention. For the future, beyond the doubling of the present data set which is yet to be exploited during the present run we look forward to a bright and exciting future with an upgraded detector and a factor of twenty increase in integrated luminosity.

8 Acknowledgements

I would like to thank all my colleagues on DØ , who obtained the results described herein. I would also like to thank the organisers of the conference whose invitation gave me the chance to discuss physics in a wonderful setting on my first trip south of the equator. The hospitality has been superb.

References

[1] A list of DØ journal and conference publications is maintained on the World Wide Web at *http* : *//d0sgi0.fnal.gov/publications_talks/publications_talks.html*. Fermilab Note 640, "The Standard Model and Beyond: Physics with the DØ Experiment" Editor: Paul Quintas, Contributors: Stefan Gruenendahl, Terry Heuring, Thorsten Huehn, Greg Landsberg, Lee Sawyer, Gordon Watts.

[2] The collected reprints of publications in Physical Review and Physical Review Letters from the CDF Collaboration can be obtained as Fermilab-Pub-95/248-E (1995)

[3] S. Abachi *et al.*, Nucl. Instr. and Meth. A338, 185 (1994).

[4] S. Abachi *et al.*, Phys. Rev. Letters 74, 3548 (1995).

[5] Gilvan Alves, "b Quark Physics at DØ ." Talk presented at this conference.

[6] S. Abachi *et al.*, Phys. Rev. Letters 72, 2332 (1994).

[7] S. Abachi *et al.*, to be published in Phys. Rev. Letters.

[8] S. Abachi *et al.*, Phys. Rev. Letters 75, 1034 (1995).

[9] S. Abachi *et al.*, Phys. Rev. Letters 75, 1028 (1995).

[10] S. Abachi *et al.*, Phys. Rev. Letters 75, 1023 (1995).

[11] Phys. Rev. Letters 75, 1456 (1995).

[12] F. Abe *et al.*, Phys Rev. Letters 74, 2626 (1995).

[13] S. Abachi *et al.*, Phys Rev. Letters 74, 2632 (1995).

[14] S. Abachi *et al.*, Phys. Rev. D52, 4877 (1995).

[15] DØ Collaboration, S. Snyder, in International Europhysi Europhysics Conference on High Energy Physics (HEP 95), Brussels, 1995.

[16] K. Kondo, J. Phys. Soc. Japan 57, 4126(1988), R. H. Dalitz and G. R. Goldstein, Phys. Rev. D45, 1531 (1992).

[17] S. Abachi *et al.*, Phys. Rev. Letters 75 618 (1995).

[18] OPAL Collaboration, OPAL Physics Note 181(Jul 1995), submitted to the EPS-HEP Conference, Brussels, 27 July- 2 August 1995(EPS0278) and The Lepton Photon Symposium, Beijing, 10-15 August, 1995. DELPHI Collaboration, DELPHI Note 95-89-PHYS-524 (Jul 1995), submitted to the EPS-HEP Conference, Brussels, 27 July- 2 August 1995(EPS0570)

[19] S. Abachi *et al.*, to be published in Phys. Rev. Letters. (FERMILAB-PUB-95/380-E)

[20] S. Abachi *et al.*, to be published in Phys. Rev. Letters. (FERMILAB-PUB-95/385-E)